Cyclostationarity-Based Detection of Randomly Arriving or Departing Signals

Y. Lee[1], S. R. Lee[2], S. Yoo[3], H. Liu[4] and S. Yoon*[5]

[1] Samsung Electronics
Suwon, Korea
[2] Department of Information and Electronics Engineering
Mokpo National University
Muan, Korea
[3] Department of Electronics Engineering
Konkuk University
Seoul, Korea
[4] School of Electrical Engineering and Computer Science
Oregon State University
Corvallis, OR, USA
[5] College of Infomation and Communication Engineering
Sungkyunkwan University
Suwon, Korea
*syoon@skku.edu

ABSTRACT
This paper addresses the problem of detection of randomly arriving or departing primary user (PU) signals in cognitive radio systems. The detection problem of the dynamic PU signal is modeled as a binary hypothesis testing problem where the PU signal might randomly depart or arrive during the sensing period. Then, we detect the cyclostationarity of the PU signal using a test statistic derived from the spectral autocoherence function in dynamic PU signal environments. Numerical results show that the proposed scheme offers an improved spectrum sensing performance than the conventional energy detector for dynamic PU environments.

Keywords: Spectrum sensing, CR, cyclostationarity, dynamic primary user signals.

1. Introduction

The rapid growth of broadband wireless applications makes the frequency spectrum a scarce resource [1], [2], and thus, its more efficient use is needed [3]. The cognitive radio (CR) is a promising technology to exploit underutilized spectrum in an opportunistic manner and the spectrum sensing technique identifying spectrum holes is one of the most important techniques in CR [4]-[6]. Until now, various spectrum sensing techniques have been developed under static traffic circumstances where the spectrum band is assumed to be occupied by the primary user (PU) or vacant during the whole sensing period [7], [8]. In practical cases, however, the PU signal could depart or arrive during the sensing period, especially when a long sensing period is used to achieve a good sensing performance, or when the spectrum sensing is performed for a high traffic network, In dynamic PU signal environments, the performances of the conventional spectrum sensing techniques have been found to be degraded severely [9]. Although a spectrum sensing technique [10] was proposed based on the energy detection approach for dynamic PU signals, it performs poorly when the signal-to-noise ratio (SNR) is low.

In this paper, we propose a novel spectrum sensing scheme based on the cyclostationarity approach for randomly arriving or departing signals, which is referred to as the dynamic PU signals. We first formulate the spectrum sensing problem in dynamic PU signal environments as a binary hypothesis testing problem and develop the corresponding generalized likelihood ratio (GLR). Obtaining an estimate of spectral autocoherence function (SAF) of the PU signal and applying it to the GLR, we propose a test statistic for spectrum sensing in dynamic PU signals. The proposed cyclostationarity-based scheme is expected to perform better than the conventional energy detection-based scheme of [10], since the cyclostationarity-based detection has an advantage over the energy detection approach in that its detection performance is generally better than that of the energy detection approach, and also, it can distinguish the PU signal from the interference unlike the energy detection approach.

2. System model

In the conventional researches without considering the dynamic behavior of PU signals, the received signal $y[n]$ in the absence of noise can be depicted as shown in Figure 1. However, the PU signals can randomly depart or arrive during the sensing period as shown in Figure 2, where the event of random departure (random arrival) is assumed to occur between the samples $J_0\left(J_1\right)$ and $J_0+1\left(J_1+1\right)$. The goal of the spectrum sensing is to estimate the existence of the PU signal after $n = N$ by detecting the samples in the sensing period (that is n = 1, 2, ..., N). For example, in the random departure case, the PU signal is absent after the sensing period meanwhile the PU signal is present after the sensing period in the random arrival case.

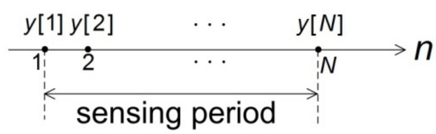

(a) When the PU signal is absent.

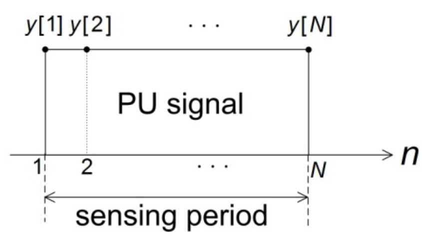

(b) When the PU signal is present.

Figure 1. The received signal model without considering the dynamic behavior of PU signals.

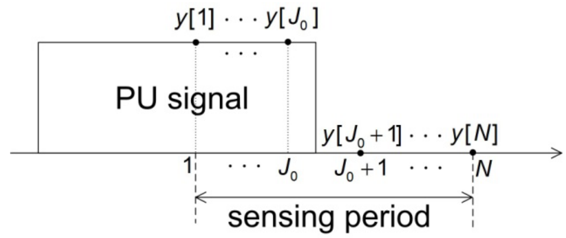

(a) Random departure.

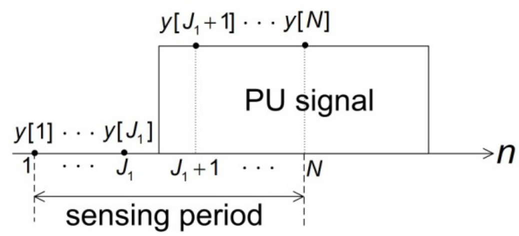

(b) Random arrival.

Figure 2. The received signal model for randomly departing or arriving PU signals.

We model the spectrum sensing problem in dynamic PU signals where the PU randomly departs or arrives during the sensing period of CR user as a binary hypothesis testing problem: Given the received signal, a decision is to be made between the null hypothesis H_0 and the alternative hypothesis H_1 defined as

$$H_0:\ y[n]=\begin{cases} x[n]+w[n],\ \text{for } n=1,2,\ldots,J_0, \\ w[n],\ \text{for } n=J_0+1,J_0+2,\ldots,N \end{cases} \tag{1}$$

and

$$H_1:\ y[n]=\begin{cases} w[n],\text{for } n=1,2,\ldots,J_1, \\ x[n]+w[n],\ \text{for } n=J_1+1,J_1+2,\ldots,N, \end{cases} \tag{2}$$

respectively, where and represent the sample of the baseband equivalent of the received and PU signals, respectively, $w\left[n\right]$ represents the nth sample of an additive white Gaussian noise (AWGN) with mean zero and variance σ^2, and N is the number of samples available during the sensing period. Under the hypothesis H_0, the random departure of the PU occurs between the J_0th and (J_0+1)th samples, on the other hand, under the hypothesis H_1, the random arrival of the PU occurs between the J_1th and (J_1+1)th samples.

3. Proposed scheme

Applying the GLR test to the binary hypothesis model of Eqs. 1 and 2 gives the following decision rule

$$\sum_{n=J_0+1}^{N} y^2[n] - \sum_{n=1}^{J_1} y^2[n] \underset{H_0}{\overset{H_1}{\gtrless}} \gamma', \tag{3}$$

where γ' is a predetermined threshold. To exploit the cyclostationarity of the received PU signal, in Eq. 3, we replace $y[n]$ with the SAF $\rho_y^\alpha(f)$ defined as [11]

$$\rho_y^\alpha(f) = \frac{S_y^\alpha(f)}{\left[S_y(f+\alpha/2)S_y(f-\alpha/2)\right]^{1/2}}, \tag{4}$$

where α is a cyclic frequency, $S_y(f)$ is the PSD of $y(t)$, and

$$S_y^\alpha(f) = \int_{-\infty}^{\infty} R_y^\alpha(\tau) e^{-j2\pi f\tau} d\tau \tag{5}$$

is the spectral correlation density (SCD) function defined as the Fourier transform of $R_y^\alpha(\tau)$, where $R_y^\alpha(\tau)$ is the cyclic autocorrelation function and expressed as

$$R_y^\alpha(\tau) = \lim_{A\to\infty} \frac{1}{A} \int_{-A/2}^{A/2} y\left(t+\frac{\tau}{2}\right) y^*\left(t-\frac{\tau}{2}\right) e^{-j2\pi\alpha t} dt, \tag{6}$$

where $(\bullet)^*$ is the conjugation operation. From Eqs. 4 and 5, we can see that the SAF is the normalized version of the SCD.

Since $\rho_y^\alpha(f)$ is the SAF of a continuous signal $y(t)$, we cannot replace the discrete value $y^2[n]$ of Eq. 3 with $\left(\rho_y^\alpha(f)\right)^2$ directly. Thus, we employ the discrete estimate $\left|\hat{\rho}_y^\alpha(f)\right|^2$ of the squared magnitude of the SAF obtained as

$$\left|\hat{\rho}_y^\alpha(f)\right|^2 = \frac{\left|\sum_{n=1}^{N} u[n]v^*[n]\right|^2}{\sum_{n=1}^{N}|u[n]|^2 \sum_{n=1}^{N}|v[n]|^2} \tag{7}$$

to replace $y^2[n]$ of Eq. 3, where $u[n] = y[n]e^{j\pi(f-\alpha/2)n}$ and $v[n] = y[n]e^{j\pi(f+\alpha/2)n}$ are the frequency-shifted versions of $y[n]$. Now, replacing $y^2[n]$ with Eq. 7 yields

$$\sum_{n=J_0+1}^{N} \left|\hat{\rho}_y^\alpha(f)\right|^2 - \sum_{n=1}^{J_1} \left|\hat{\rho}_y^\alpha(f)\right|^2 \underset{H_0}{\overset{H_1}{\gtrless}} \gamma, \tag{8}$$

where γ is a threshold for the decision rule Eq. 8. It should be noted that the values of J_0 and J_1 change randomly depending on the behavior of the PU, and thus, the test statistics unconditional for random departure and arrival are obtained by taking the expectation over the left side of Eq. 8 with respect to J_0 and J_1, respectively. Generally, the number of events occurring randomly over a period of time is well modeled by a Poisson process [12], and thus, we assume that the departure or arrival of the PU follows a Poisson process. Then, we have

$$\Pr\{J_0\} = [1-e^{-\lambda_d T}]\cdot[e^{-\lambda_d T}]^{J_0}, \tag{9}$$

and

$$\Pr\{J_1\} = [1-e^{-\lambda_a T}]\cdot[e^{-\lambda_a T}]^{J_1}, \tag{10}$$

where λ_d, λ_a, and T represent the departure rate, arrival rate, and sampling interval, respectively. Using Eqs. 9 and 10, finally, we obtain the unconditional test statistics

$$T_d = \left|\sum_{J_0=0}^{N-1}[1-e^{-\lambda_d T}]\cdot[e^{-\lambda_d T}]^{J_0} \sum_{n=J_0+1}^{N} u[n]v^*[n]\right|^2 \Big/ \left[\sum_{J_0=0}^{N-1}[1-e^{-\lambda_d T}]\cdot[e^{-\lambda_d T}]^{J_0} \sum_{n=J_0+1}^{N} |u[n]|^2\right]$$

$$/\left[\sum_{J_0=0}^{N-1}[1-e^{-\lambda_d T}]\cdot[e^{-\lambda_d T}]^{J_0}\sum_{n=J_0+1}^{N}\left|v[n]\right|^2\right]$$
$$=\frac{\left|\sum_{n=1}^{N}[1-e^{-\lambda_d Tn}]u[n]v^*[n]\right|^2}{\sum_{n=1}^{N}[1-e^{-\lambda_d Tn}]\left|u[n]\right|^2\sum_{n=1}^{N}[1-e^{-\lambda_d Tn}]\left|v[n]\right|^2} \tag{11}$$

for the random departure of the PU, and similarly,

$$T_a=\frac{\left|\sum_{n=1}^{N}[1-e^{-\lambda_a Tn}]u[n]v^*[n]\right|^2}{\sum_{n=1}^{N}[1-e^{-\lambda_a Tn}]\left|u[n]\right|^2\sum_{n=1}^{N}[1-e^{-\lambda_a Tn}]\left|v[n]\right|^2} \tag{12}$$

for the random arrival of the PU.

From Eqs. 11 and 12, we can see that the term $[1-e^{-\lambda_d Tn}]$ ($[1-e^{-\lambda_a Tn}]$) becomes larger as the value of n increases, which implies that the cross-correlation $\left|\sum_{n=1}^{N}[1-e^{-\lambda_d Tn}]u[n]v^*[n]\right|^2$ ($\left|\sum_{n=1}^{N}[1-e^{-\lambda_a Tn}]u[n]v^*[n]\right|^2$) and the autocorrelations $\sum_{n=1}^{N}[1-e^{-\lambda_d Tn}]\left|u[n]\right|^2$ and $\sum_{n=1}^{N}[1-e^{-\lambda_d Tn}]\left|v[n]\right|^2$ ($\sum_{n=1}^{N}[1-e^{-\lambda_a Tn}]\left|u[n]\right|^2$ and $\sum_{n=1}^{N}[1-e^{-\lambda_a Tn}]\left|v[n]\right|^2$) are correlation operations that give a larger weight on the samples with a large value of n. Figure 3 shows a block diagram to obtain the test statistic T_d. As $T_d = T_a$ when $\lambda_d = \lambda_a$, we can employ either T_d or T_a as a test statistic of the proposed scheme assuming that $\lambda_d = \lambda_a$.

4. Numerical results

In this section, we compare the spectrum sensing performance of the proposed scheme with that of the conventional scheme of [10] in terms of the receiver operating characteristic (ROC) and detection probabilities. We assume the following parameters: $N = 100$, $\lambda_d T = \lambda_a T = 1$, $\alpha = 2f_c$, $P_{fa} = 0.01, 0.03, 0.05, 0.15, 0.4$, and 1, and a PU signal modulated by the binary phase shift keying with a carrier frequency f_c of 100 Hz. The threshold is determined from the false alarm probabilities [13], and it is assumed that one of the random departure and arrival is chosen randomly with equal probability.

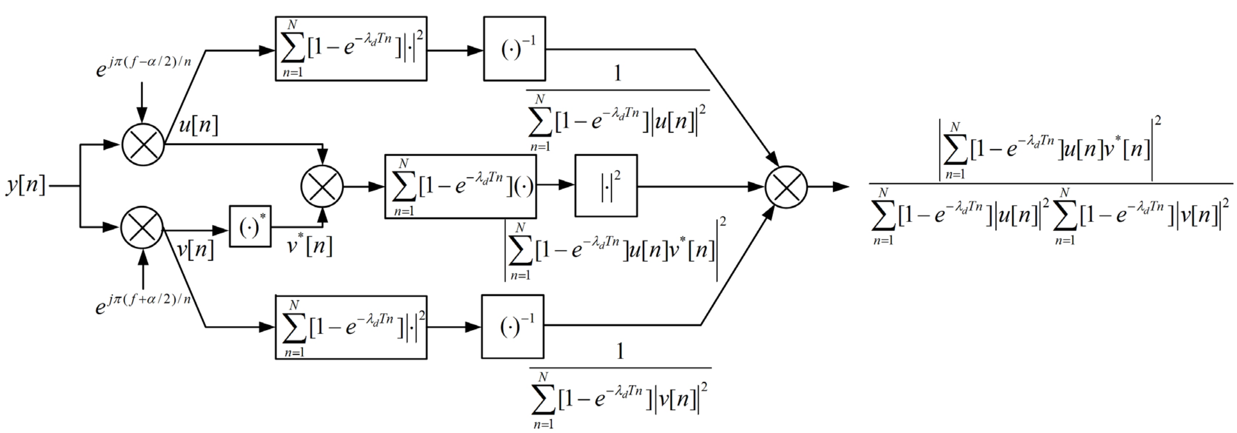

Figure 3. The test statistic T_d of the proposed scheme.

Figure 4 shows the ROC curves of the proposed and conventional schemes over an AWGN channel in dynamic PU signals with the SNR value of -15, -10, -5, and 0 dB, where P_d represents the detection probability defined as $\Pr(H_1|H_1)$: Here, the SNR is defined as σ_s^2/σ^2, where σ_s^2 is the variance of the PU signal. From the figure, it is clearly observed that the proposed scheme provides a significant performance improvement over the conventional scheme, and the performance improvement becomes more noticeable as the SNR increases.

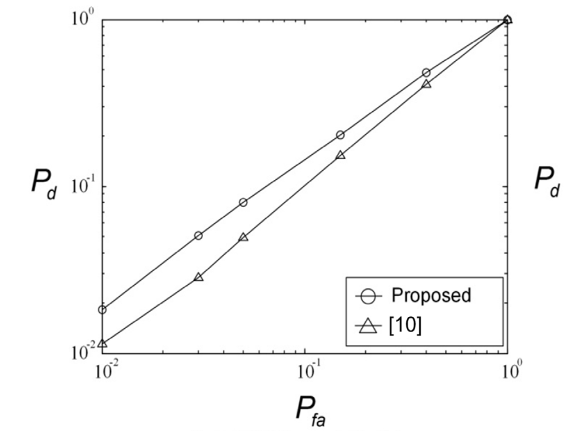

(a) SNR= -15 dB.

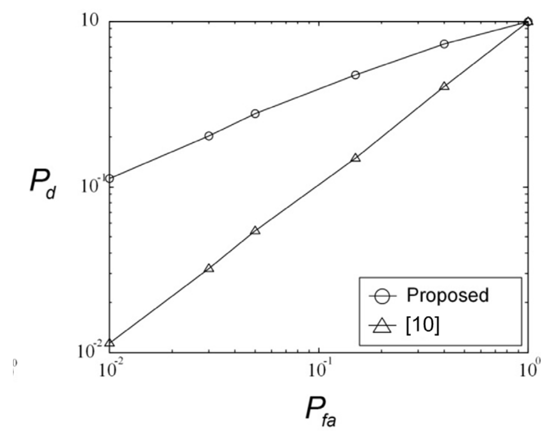

(b) SNR= -10 dB.

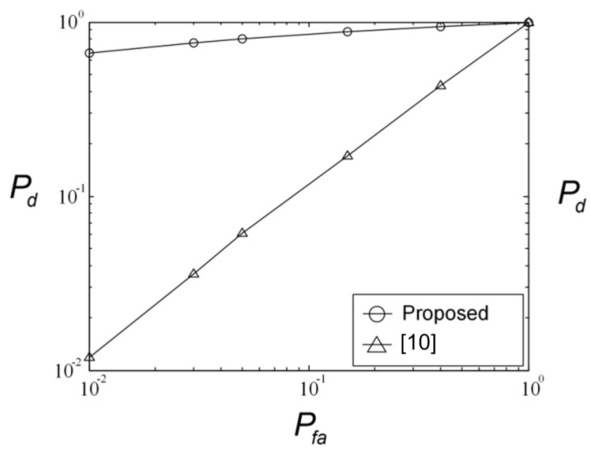

(c) SNR= - 5 dB.

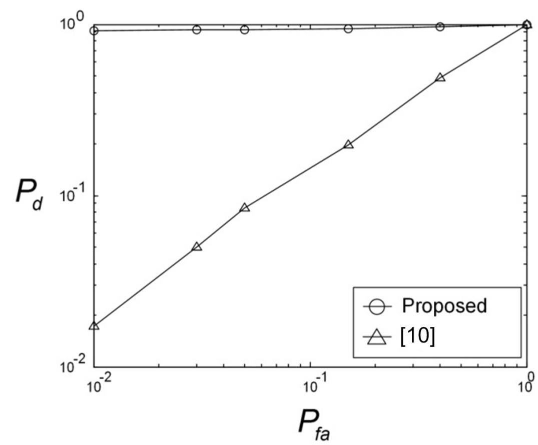

(d) SNR= 0 dB.

Figure 4. ROC curves of the proposed and conventional schemes over AWGN channel in dynamic PU signals when SNR = -15, -10, -5, and 0 dB.

Figure 5 shows the detection probabilities of the proposed and conventional schemes over AWGN channel in dynamic PU signals as a function of P_{fa} when $P_{fa} = 0.15$, 0.05, and 0.01. From the figure, we can see that the proposed scheme has a better detection performance than the conventional scheme in the SNR range of -10 ~ 10 dB. This is due to the fact that cyclostationarity of the signal is easily distinguishable regardless of the SNR value since the AWGN is not a cyclostationary process, whereas it is difficult for the conventional scheme to detect the signal energy correctly in low SNR environments. Moreover, the performance deference between the proposed and conventional schemes becomes more pronounced as the value of the false alarm probability decreases.

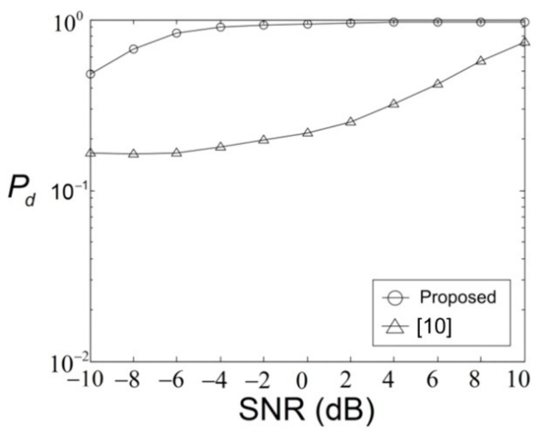

(a) P_{fa} = 0.15.

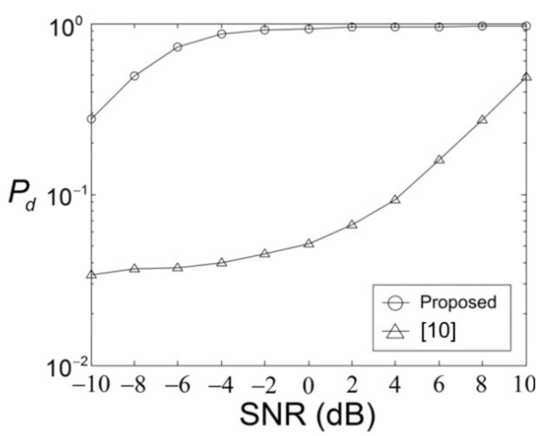

(b) P_{fa} = 0.05.

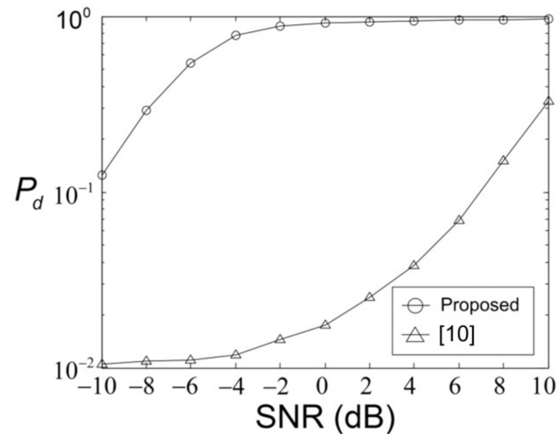

(c) P_{fa} = 0.01

Figure 5. Detection probabilities of the proposed and conventional schemes over AWGN channel in dynamic PU signals as a function of SNR when $P_{fa} = 0.15$, 0.05, and 0.01.

Figures 6 and 7 show the performances of the proposed and conventional schemes over multipath Rayleigh fading channels in terms of ROC and detection probabilies, respectively. For simulations, we assume that the multipath fading environments consist of three paths with exponential power delay profile (PDP), where the PDP p_k for the kth path is expressed as

$$p_k = \exp(-k\tau) / \sum_{k=0}^{2} \exp(-k\tau) \qquad (13)$$

and τ denotes the relative timing difference between the paths [14]. In this paper, we assume that the paths are equally spaced with interval $\tau = N/3$.

Figure 6 shows the ROC curves of the proposed and conventional schemes over multipath Rayleigh fading channels in dynamic PU signal environments with the SNR value of -15, -10, -5, and 0 dB. From the figure, it is clearly observed that the proposed scheme exhibits a better ROC performance than the conventional scheme in multipath Rayleigh fading channels as well. Moreover, the performance improvement over the conventional scheme becomes more significant as the value of SNR increases.

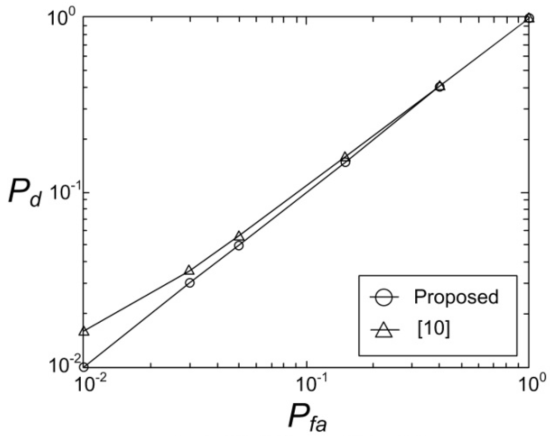

(a) SNR = -15 dB.

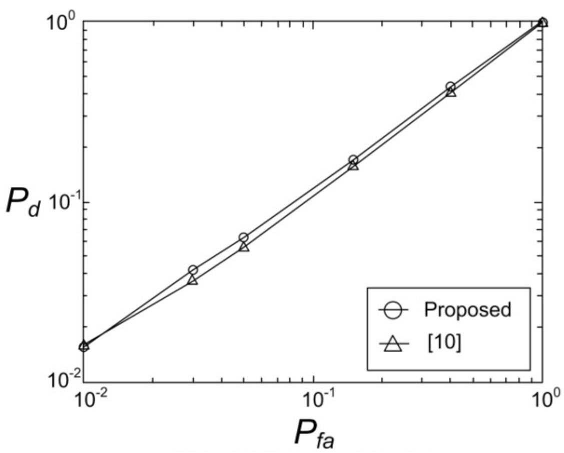

(b) SNR = -10 dB.

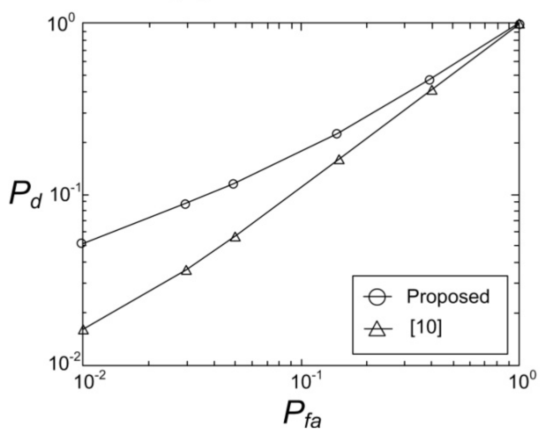

(c) SNR = -5 dB.

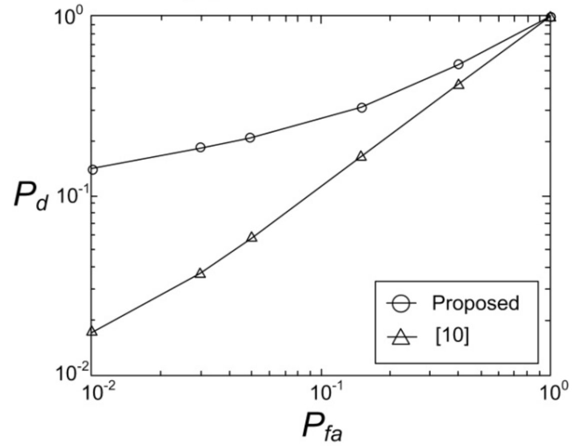

(d) SNR = 0 dB.

Figure 6. ROC curves of the proposed and conventional schemes over multipath Rayleigh fading channel in dynamic PU signals when SNR = -15, -10, -5, and 0 dB.

Figure 7 shows the detection probabilities of the proposed and conventional schemes over multipath Rayleigh fading channels in dynamic PU signal environments as a function of SNR when $P_{fa} = 0.15$, 0.05, and 0.01. From the figure, we can see that the proposed scheme provides an improved detection performance than the conventional scheme. Moreover, the performance improvement becomes more pronounced as the value of the false alarm probability decreases.

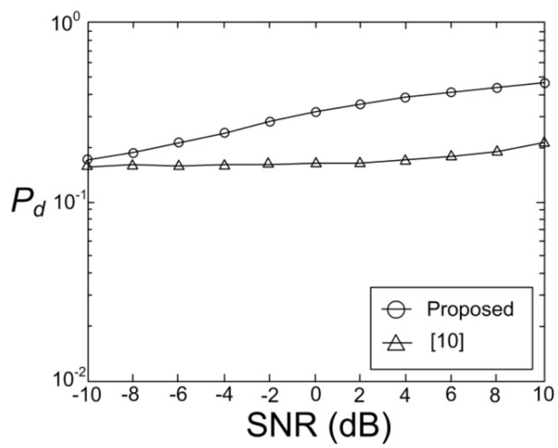

(a) P_{fa} = 0.15.

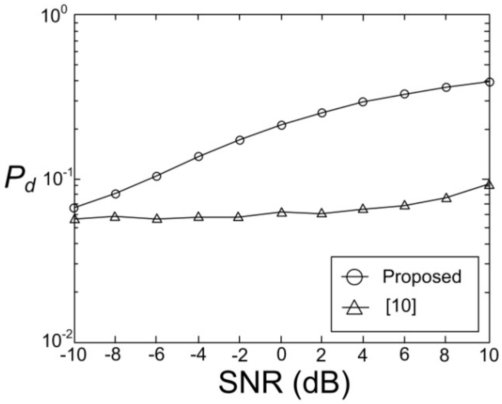

(b) P_{fa} = 0.05.

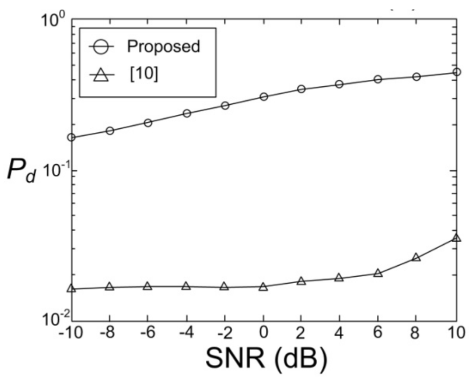

(c) P_{fa} = 0.01.

Figure 7. Detection probabilities of the proposed and conventional schemes over multipath Rayleigh fading channelsin dynamic PU signals as a function of SNR when $P_{fa} = 0.15$, 0.05, and 0.01.

We also compare the complexities of the proposed and conventional schemes in terms of the number of additions, number of real multiplications, and number of flops, where a flop is defined as a real floating point operation, and a real addition or multiplication is counted as one flop [15]. A complex addition operation is counted as two real addition operations and a complex multiplication operation consists of two real addition and four real multiplication operations.

Table 1 shows the computational complexities of the proposed and conventional schemes. From the table, we can see that the computational complexity of the proposed scheme is almost three times that of the conventional scheme; however, the complexity difference would be insignificant since the recent Intel microprocessor is ideally capable of 4 flops per clock (i.e., a 2.5-GHz Intel microprocessor has a theoretical peak performance of 10 billion flops per second) [16]. Moreover, the complexities of the proposed and conventional schemes are both in order of N, which also shows that the spectrum sensing can be achieved in a similar level of sensing time using the both spectrum sensing schemes.

Scheme	Number of real addition	Number of real multiplication	Number of flops
Proposed	$20N-2$	$24N+8$	$48N+6$
[10]	$8N-1$	$8N$	$16N-1$

Table 1. Computational complexities of the proposed and conventional schemes.

5. Conclusion

In this paper, we have proposed a cyclostationarity-based spectrum sensing scheme in the presence of randomly arriving or departing PU signals. Firstly, we have modeled the spectrum sensing problem in dynamic PU signal environments as a binary hypothesis testing problem, and then, developed the corresponding GLR. Then, we have derived a test statistic employing the SAF in the GLR. From numerical results, it has been demonstrated that the proposed scheme provides a significant performance improvement over the conventional scheme in terms of the ROC and detection probability in both AWGN and multipath Rayleigh fading channels while maintaining a similar level of computational complexity compared with that of the conventional scheme.

Acknowledgments

This research was supported by the National Research Foundation (NRF) of Korea under Grant 2014R1A5A1011478 and by the Convergence Information Technology Research Center (C-ITRC) support program supervised by the National IT Industry Promotion Agency (NIPA) under Grant NIPA-2014-H0401-14-1009 with funding from the Ministry of Science, ICT and Future Planning (MSIP), Korea, and by Priority Research Centers Program through the NRF of Korea under Grant 2009-0093828 with funding from the Ministry of Education, Science and Technology.

References

[1] J. Sánchez et al., “Mean receiver power prediction for indoors 802.11 WLANs using the ray tracing technique,” Journal of Applied Research and Technology, vol. 5, no. 1, pp. 33-48, 2007.

[2] N. C. Wang et al., “RSVP extensions for seamless handoff in heterogeneous WLAN/WiMAX networks,” Journal of Applied Research and Technology, vol. 11, no. 4, pp. 540-548, 2013.

[3] Y.-C. Lee et al., “Cryptanalysis and improvement of the robust user authentication scheme for wireless sensor networks,” International Journal of Engineering and Technology Innovation, vol. 2, no. 4, pp. 283-292, 2012.

[4] J. Mitola, “Cognitive radio: An integrated agent architecture for software defined radio,” Ph.D. dissertation, Royal Institute of Technology, Stockholm, Sweden, 1996, pp. 271-350.

[5] J. Lunden et al., “Robust nonparametric cyclic correlation-based spectrum sensing for cognitive radio,” IEEE Trans. Sig. Process., vol. 58, no. 1, pp. 38-52, 2010.

[6] Y. L. Lee et al., “Improved detection performance of cognitive radio networks in AWGN and Rayleigh fading environments,” Journal of Applied Research and Technology, vol. 11, no. 3, pp. 437-446, 2013.

[7] D. Cabric et al., “Implementation issues in spectrum sensing for cognitive radios,” in Asilomar Conference on Signals, Systems and Computers, Pacific Grove, CA, 2004, pp. 772-776.

[8] T. S. Shehata and M. El-Tanany, “A novel adaptive structure of the energy detector applied to cognitive radio networks,” in 11th Canadian Workshop on Information Theory, Ottawa, Canada, 2009, pp. 95-98.

[9] T. Wang et al., “Analysis of effect of primary user traffic on spectrum sensing performance,” in Communications And Networking, Xian, China, 2009, pp. 1-5.

[10] N. C. Beaulieu and Y. Chen, “Improved energy detectors for cognitive radios with randomly arriving or departing primary users,” IEEE Sig. Process. Lett., vol. 17, no. 10, pp. 867-870, 2010.

[11] W. A. Gardner, “Exploitation of spectral redundancy in cyclostationary signals,” IEEE Sig. Process. Mag., vol. 8, no. 2, pp. 14-36, 1991.

[12] P. Z. Peebles, “Probability, random variables and random signal principles”, New York, NY: McGraw-Hill, 2001.

[13] H. L. V. Trees, “Detection, Estimation, and Modulation Theory,” Hoboken, NJ: John Wiley & Sons, 2004.

[14] D. Chong et al., “A two-stage acquisition scheme based on multiple correlator outputs for UWB signals,” IEICE Electron. Express, vol. 8, no. 7, pp. 436-442, 2011.

[15] H. Liu et al., “A low-complexity scheduling scheme for multiuser MIMO system based on Tomlinson-Harashima precoding,” in Int. Conf. Inform. Theory and Inform. Security (ICITIS), Beijing, China, 2010, pp. 981- 984.

[16] J. Brown, “Efficient nonlinear solvers for nodal high-order finite elements in 3D,” J. Scientific Computing, vol. 45, no. 1-3, pp. 48-63, 2010.